

## Article

# The Effect of the Artificial Reef on the Structure and Function of Sediment Bacterial Community

Fei Tong <sup>1,2,3,4,5,\*</sup> , Guobao Chen <sup>1,2,3,4,5</sup>, Xue Feng <sup>1,2,3,4,5</sup>, Yan Liu <sup>1,2,3,4,5</sup> and Pimao Chen <sup>1,2,3,4,5</sup>

- <sup>1</sup> South China Sea Fisheries Research Institute, Chinese Academy of Fishery Sciences, Guangzhou 510300, China
- <sup>2</sup> Shenzhen Base of South China Sea Fisheries Research Institute, Chinese Academy of Fishery Sciences, Shenzhen 518121, China
- <sup>3</sup> Key Laboratory of Marine Ranching, Ministry of Agriculture and Rural Affairs, Guangzhou 510300, China
- <sup>4</sup> Scientific Observing and Experimental Station of South China Sea Fishery Resources and Environment, Ministry of Agriculture and Rural Affairs, Guangzhou 510300, China
- <sup>5</sup> National Digital Fisheries (Marine Ranching) Innovation Sub-Center, Guangzhou 510300, China
- \* Correspondence: tongfei@scsfri.ac.cn

**Abstract:** The bacterial community in sediment is sensitive to artificial disturbance, and they respond differently to human disturbance, such as changing the nutrient cycling and energy flow in marine ecosystems. However, little is known about the dynamics and distribution of bacterial community structures in marine sediments and potential biogeochemical functions during the long-time succession in marine ranching. In the present study, we compared the dynamics of the bacterial composition and potential biogeochemical functions of sediment to ten years (TR) and one-year new artificial reef (NR) areas using metagenomic next-generation sequencing technology. Results revealed that NR reduces the Pielou's evenness and Shannon index. Similarly, nonmetric multidimensional scaling showed that the beta diversity of sediment bacterial communities in NR significantly differed between TR and non-artificial reef areas. Previously, TR biomarkers were frequently associated with organic matter decomposing and assimilating in the organically enriched sediments (i.e., *Acinetobacter*). The soluble reactive phosphate (SRP) and total phosphorus (TP) concentrations were thought to be the primary driving forces in shaping the microbial community in sediment. *Pseudomonas*, *Lactobacillus*, and *Ralstonia* have a significant positive correlation with SRP, TP, nitrate, and TN, but a negative association with pH, Salinity, Hg, and depth. NR was found to have more negative correlation nodes, indicating that taxa face more competition or predation press. *Vibrio* served as the module-hubs in the network in all areas. In addition, chemoheterotrophy, aerobic chemoheterotrophy, and fermentation were the three most prominent functions of the three areas, accounting for 59.96% of the relative abundance of the functional annotation. Different bacteria in sediments may change the amount of biogeochemical cycle in the marine ranching ecosystem. These findings can increase our understanding of the succession of the microecosystem for the marine ranching sedimentary environment by revealing how artificial reefs affect the indigenous sediment bacterial community and their responses to environmental variation.

**Keywords:** marine ranching; artificial reef; community structure; keystone taxa; FAPROTAX



**Citation:** Tong, F.; Chen, G.; Feng, X.; Liu, Y.; Chen, P. The Effect of the Artificial Reef on the Structure and Function of Sediment Bacterial Community. *Sustainability* **2022**, *14*, 14728. <https://doi.org/10.3390/su142214728>

Academic Editors: Peter A. Bowler, Wen Xiong, Zhongxin Wu, Xiaoyu Li and Dongkui Gao

Received: 28 September 2022

Accepted: 6 November 2022

Published: 8 November 2022

**Publisher's Note:** MDPI stays neutral with regard to jurisdictional claims in published maps and institutional affiliations.



**Copyright:** © 2022 by the authors. Licensee MDPI, Basel, Switzerland. This article is an open access article distributed under the terms and conditions of the Creative Commons Attribution (CC BY) license (<https://creativecommons.org/licenses/by/4.0/>).

## 1. Introduction

China has been practicing marine ranching since the late 1970s, primarily through constructing artificial reefs (ARs) and stock enhancement [1]. In 1979, China installed 26 experimental small individual ARs along the coast of Guangxi [2]. By 2016, the total amount of funds used for marine ranching construction in China had reached 5.58 billion yuan, more than 200 marine ranches had been built, and more than 60 million cubic meters of ARs had been installed [3,4]. The primary goal of marine ranching construction is to increase marine fishery resources [1]. Marine ranching may provide a viable solution for

reducing wastewater and overfishing as well as achieving aquaculture sustainability [5]. By 2021, 153 national-level nearshore marine ranching areas had been approved for development. The Ministry of Agriculture and Rural Affairs invested more than 2.9 billion yuan between 2016 and 2021 to support 153 artificial reef construction projects, totaling more than 50 million m<sup>3</sup> of reefs.

Concrete is a widely used material for ARS construction worldwide because of its stability, ease of shaping into various structures and sizes, and high biological fixation rate [6]. Tons of concrete reefs on the sea floor changed the flow field of the sea floor [7]. The complex flow field near ARS not only provides a suitable activity area for various marine organisms but also promotes the exchange of various nutrients and enhances the ecological effect of ARS. The transport and exchange of sediment nutrients can be promoted by upwelling [8]. Long-term exposure to seawater caused chemical and mineralogical alteration in some concrete regions. Calcium hydroxide ions, iron, and silicate in ARS were transported to the external environment [9,10].

Microbial communities in sediments play an important role in organic remineralization, helping to maintain biogeochemical cycles, release nutrients, and emit greenhouse gases [11,12]. As primary producers, these prokaryotes form an indispensable foundation of the food web of the ARS ecosystem, supporting a diverse range of benthic life, from microbial consumers to animals like zooplanktons, clams, mussels, and shrimps [13]. Bacterial communities can exhibit spatial or temporal patterns and are influenced by different environmental parameters and human activities [14,15], such as artificial reef construction in marine ranching [16]. In recent decades, a long-standing research focus has been on microbial communities' distribution patterns in marine sediments [17]. Sediments microbial communities are sensitive to environmental changes, and bacterial communities respond differently to disturbance [16,18].

The Beibu Gulf is located in the south of the Guangxi province. It is a traditional and economically significant subtropical fishery area [19]. Due to the discharge of urban and industrial wastewater and overfishing, the marine environment has deteriorated, and fishery resources have been depleted [20]. The local government started building reef-throwing marine ranching ten years ago and recently began building national-level marine ranching [21]. However, the studies related to the bacterial community of sediment in response to ARS are still insufficient [16,22]. Thus, the present study aimed to address how ARS of different ages (1) shape the bacterial composition in the surrounding sediment and (2) determine whether bacteria function in response to environmental features to provide context for their potential as drivers of bacterial biodiversity in sediment.

## 2. Materials and Methods

### 2.1. Study Area and Samples Collection

The present study was conducted at the southern sea area of Yingtan in the Beibu Gulf in March 2022. The water depth in this area is approximately 11–20 m. We took samples from a ten-year artificial reef area (TR), a one-year new artificial reef area (NR), and a control area (CR) without reefs. The ARs are concrete cubes with 4 m side lengths. Overlying water and sediment samples were collected from 12 sites (Figure 1). Sampling sites were near the artificial reefs. Samples were collected at 250–300 m intervals along the center of each area. At each site, triplicate superficial sediments (0–10 cm mud samples) were collected on the sediment surface at 12 sites using a manual Van Veen dredge [12,23]. The sediment samples were sieved with a 2 mm mesh to remove stones and plant roots before being sealed in sterile plastic bags [24]. The sieved sediment samples were flash-frozen and kept on boards in liquid nitrogen before being stored at  $-80\text{ }^{\circ}\text{C}$  in the laboratory [25]. Overlying water samples were collected with Van Dorn bottles washed with 10% HCl and stored in triplicate flasks at  $-4\text{ }^{\circ}\text{C}$  in a cooler [12].

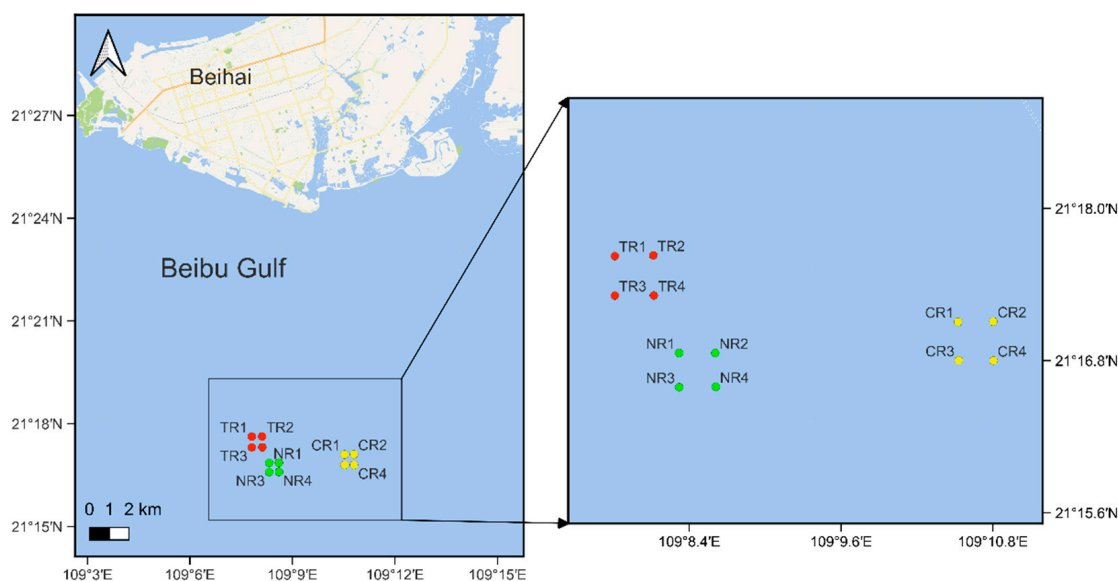


**Figure 1.** Locations of sampling sites in the marine ranching of the Beibu Gulf, China. TR: Ten-year artificial reef area; NR: one-year new artificial reef area; CR: control area (CR) without reefs.

## 2.2. Physical and Chemical Parameters

For environmental factor analyses, overlying water temperature (T), pH, salinity, and dissolved oxygen (DO) were determined in situ using a portable water quality analyzer (6600EDS, YSI, Los Gatos, CA, USA). A Secchi disk was used to measure water transparency in Secchi depth [16]. Within 24 h of sampling, ammonium ( $\text{NH}_4^+$ ), nitrate ( $\text{NO}_3^-$ ), nitrite ( $\text{NO}_2^-$ ), total nitrogen (TN), chemical oxygen demand (COD<sub>Cr</sub>), chlorophyll a (chl a), total phosphorus (TP), and concentration of soluble reactive phosphate (SRP) were determined using a spectrophotometer (cary100, varian, Palo Alto, CA, USA) according to the Marine Monitoring Code Standard GB 17378–2007.

The total organic carbon (TOC) in sediment was determined using the potassium dichromate volumetric method. Heavy metals (Cu, Pb, Zn, As, Hg and Cd) in sediment were assessed by atomic absorption spectrophotometry (Z-2010, Hitachi, Tokyo, Japan) [26]. As and Hg were determined by atomic fluorescence photometer (AFS-8520, Haiguang, Beijing, China). The pH of the sediment was measured using a pH meter (PHS-25CW, Bante, Shanghai, China) at 1/5 (*w/v*) of sediment to solution ratio in deionized water [27]. All sediment samples were collected, preserved, transported, and detected as per the National Specification for Marine Monitoring (GB 17378–2007) [16].

## 2.3. DNA Extraction and PCR Amplification

Total genomic DNA from sediment samples was extracted using a modified CTAB method [12]. DNA concentration and purity were assessed on 1% agarose gels. DNA was diluted to 1 ng/ $\mu\text{L}$  using sterile water according to the concentration. The V4 variable region of 16S rDNA genes of distinct regions was amplified using a specific primer (515FmodF–806RmodR) with the barcode, as previously described [28]. All PCR reactions used 15  $\mu\text{L}$  of Phusion<sup>®</sup> High-Fidelity PCR Master Mix (New England Biolabs), 2  $\mu\text{M}$  of forward and reverse primers, and about 10 ng template DNA. Thermal cycling consisted of 3 min of initial denaturation at 94 °C, followed by 30 cycles of denaturation at 94 °C for 30 s, annealing at 53 °C for 40 s, and elongation at 72 °C for 40 s [29]. To ensure successful amplification, mix the same volume of 1XTAE buffer with PCR products and perform electrophoresis on 2% agarose gel for detection. PCR products were mixed in equal ratios. The mixture of PCR products was then purified using the Qiagen Gel Extraction Kit (Qiagen, Hilden, Germany).

#### 2.4. Illumina NovaSeq Sequencing

The sequencing libraries were generated using TruSeq<sup>®</sup> DNA PCR-Free Sample Preparation Kit (Illumina, San Diego, CA, USA) following the manufacturer's instruction, and index codes were added. The Qubit<sup>®</sup> 2.0 Fluorometer (Thermo Scientific, Waltham, MA, USA) was used to evaluate the library quality. Finally, the library was sequenced on an Illumina NovaSeq 6000 platform, yielding 250 bp paired-end reads.

#### 2.5. Bioinformatics Analysis

The analysis was performed using the "Atacama soil microbiome tutorial" from Qiime2docs and customized program scripts (<https://docs.qiime2.org/2022.2/>, accessed on 1 June 2022). A program called Qiime tools import was used to import raw data FASTQ files into the format that could be used by QIIME2. Amplicon sequence variant feature tables (ASVs) are generated by quality filtering and trimming demultiplexed sequences, denoising, and merging them. After that, the QIIME2 dada2 plugin was used to identify and remove the chimeric sequences [30]. The QIIME2 feature-classifier plugin was then used to align ASV sequences to a pre-trained Greengenes Database 13.8 100% database (trimmed to the V4 region bound by the 515FmodF/806RmodR primer pair) to generate the taxonomy table [25,31,32]. The QIIME2 feature-table plugin filters out any contaminating mitochondrial and chloroplast sequences. Appropriate methods such as analysis of community similarities (ANOSIM), analysis of composition of microbiomes (ANCOM), Kruskal–Wallis, and LEfSe were used to identify taxa that differed significantly from phylum to genus across samples and sea areas [33,34]. Diversity metrics were calculated using the core-diversity plugin within QIIME2. To estimate the bacterial diversity within sea areas, feature level alpha diversity indices such as the Shannon diversity index and Pielou's evenness index were calculated. The structural variation of sediment bacterial communities across samples was investigated using beta diversity distance measurements, including Bray Curtis, and was then visualized through nonmetric multidimensional scaling (NMDS) [35]. Redundancy analysis (RDA) was used to assess the association of sediment bacterial genera characteristics in relation to environmental factors based on relative abundances of bacterial species at genus taxa levels using the R package "vegan" [36]. The network plot was used to display the associations among taxa in co-occurrence net analysis, which was performed by calculating Spearman's rank correlations between predominant taxa. The igraph packages were used for the network plots. In addition, functional annotation of prokaryotic taxa (FAPROTAX) was used to predict the potential functional characteristics of sedimental bacterial communities [14,37]. In this study, physicochemical variables and alpha diversity indices were expressed as the mean  $\pm$  standard deviation over four replications. The statistical analysis was performed using the Statistical Package for the Social Sciences (SPSS) version 23. [38]. All sequencing data are stored in the PRJNA880993 biological project.

### 3. Results

#### 3.1. Changes in Physicochemical Characteristics of Overlying Water and Sediment

Table S1 represents the 22 environmental factors collected at the 12 sampling sites in the three sea areas. The Kruskal–Wallis test was used to compare the geochemical characteristics of overlying water and sediment in different areas. Dunn's multiple posthoc tests were used to compare areas pairwise (Table S2). Overly water pH was significantly higher in NR areas than in CR (Dunn's test,  $p = 0.046$ ) and TR ( $p = 0.041$ ). However, dissolved nutrient concentrations of  $\text{NO}_3^-$ , TN, SRP, and TP were significantly higher in CR than in NR ( $p = 0.044$ ,  $0.035$ ,  $0.004$ , and  $0.004$ , respectively).

The physicochemical characteristics of the sediment samples varied significantly between sampling sites. The pH of the sediments in CR was significantly higher than in TR ( $p = 0.050$ ). However, the concentration of As in sediments for CR was significantly lower than for TR ( $p = 0.024$ ) (Table S2). In addition, the Cu content of the sediments in NR was significantly higher than that of TR ( $p = 0.044$ ), although Cu contents were all lower than the class I levels of the sediment environment quality standard (GB 18668–2002).

### 3.2. Sediment Bacterial Community Composition

Illumina Miseq sequencing of bacterial 16S rRNA gene was performed on each sediment sample. A total of 650,977 high-quality reads were identified across all samples, ranging from 48,128 to 62,576 reads per sample. The rarefaction plots were shown as a supplement to show the sequencing depth is sufficient (Figure S1). The 16S rRNA sequences obtained from sediment samples were grouped into 11,517 ASVs, belonging to 71 different phyla. Proteobacteria were the dominant phyla in all three sea areas (Figure S2), accounting for 61.58% relative abundance on average, followed by Crenarchaeota (5.07%), Desulfobacterota (4.90%), Firmicutes (4.30%), and Bacteroidota (3.78%) that accounted for 80% of the phyla. Gammaproteobacteria and Alphaproteobacteria were the predominant types of Proteobacteria identified, accounting for 60% of all the classes.

The largest number of ASVs (5126) were detected in the CR, and the least number (4513) was found in the NR. The CR and TR sites shared the largest number of ASVs (448), while the CR and NR areas shared the least (303). The Venn analysis identified 879 ASVs (7.63% of the total ASVs) that were common among the three areas (Figure 2). The ternary plots showed that the distribution of each genus in the three sea areas is uneven (Figure S3). NR and TR have some “special” genera, which are located in the corresponding tip area of the ternary graph. However, most of the genera in the sediments are located in the middle of the ternary block, primarily Proteobacteria, including a variety of ubiquitous genera, which exist in all samples.

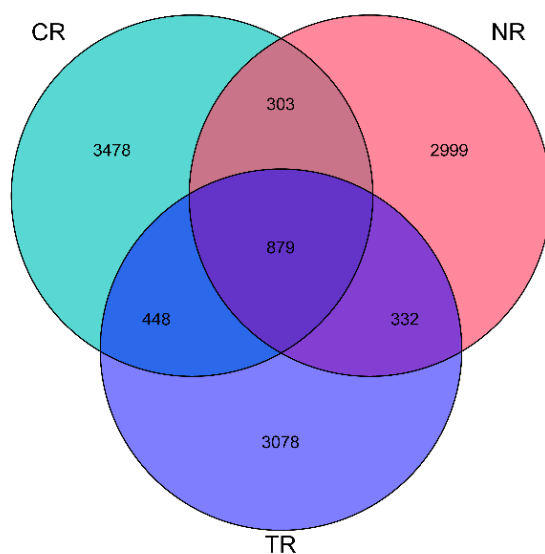


**Figure 2.** Venn diagram of the ASVs in all three areas. See Figure 1 for site abbreviations.

Sediment bacterial alpha diversity, measured by species Shannon index and Pielou’s evenness, varied significantly across research areas. The Shannon index of NR was significantly lower than that of CR ( $p = 0.029$ ) and TR ( $p = 0.029$ ). Meanwhile, the Pielou’s evenness of NR was significantly lower than that of CR (Wilcoxon test,  $p = 0.029$ ) and TR ( $p = 0.029$ ). However, the Kruskal–Wallis results revealed no statistically significant difference between CR and TR (Figure 3).

The LefSe analysis was used to identify sediment bacteria that differed significantly across three areas. In the present study, we applied a strict LDA score criterion (logarithmic LDA scores over 4.0) to the analysis. The findings revealed that six taxa were significantly enriched in 10 years of artificial reef sediment samples, including Alphaproteobacteria (class level), Rickettsiales (order level), Moraxellaceae (family level), *Acinetobacter* (genus level), Rickettsiales (family level), and *Candidatus Midichloria* (genus level). Meanwhile, three taxa were significantly enriched in NR sediments, including *Francisella* (genus level), Francisellales (family level), and Francisellales (order level). Finally, five taxa were signifi-

cantly enriched in CR sediment, including Coxiellaceae (family level), *Coxiella* (genus level), Coxiellales (order level), Lactobacillales (order level), and Bacilli (class level) (Figure 4).

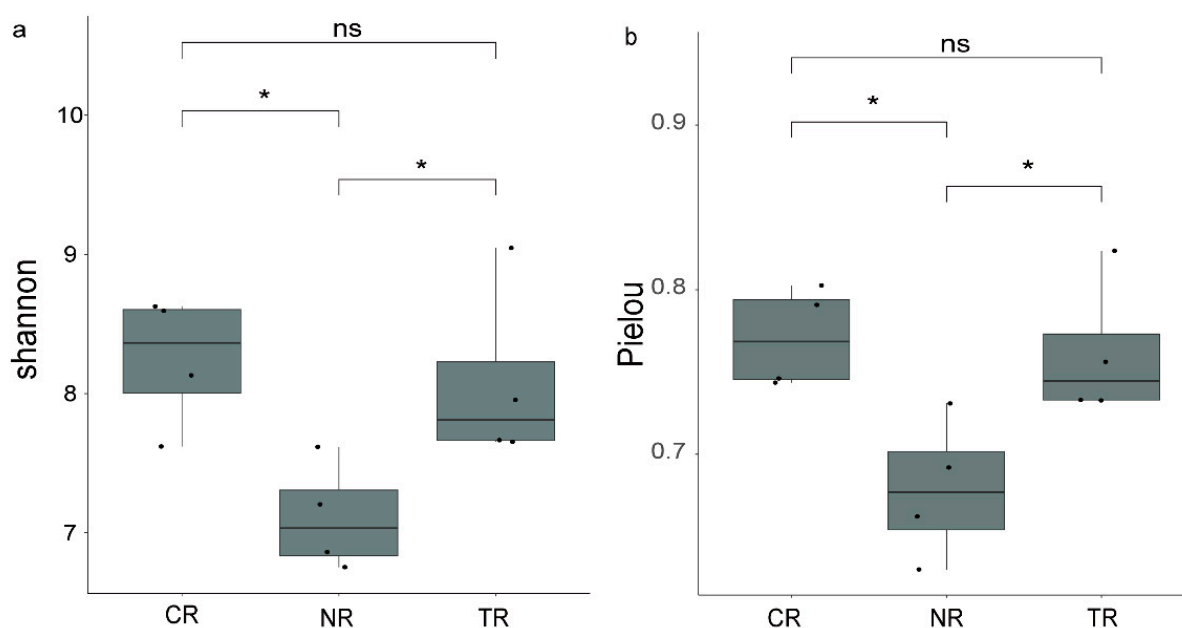


**Figure 3.** Alpha diversity analysis of the ASVs. (a) Shannon index, (b) Pielou's evenness index. Upper and lower quartile values are shown in boxes; solid horizontal lines show median values, while the maximum and minimum values are shown in upper and lower whiskers, respectively. See Figure 1 for site abbreviations. \*  $p < 0.05$ .

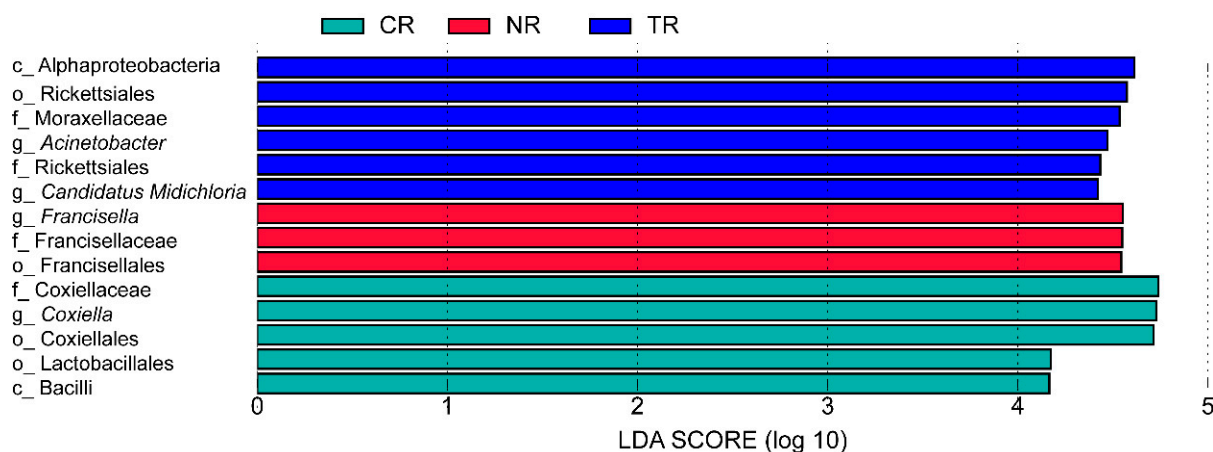


**Figure 4.** LEfSe analysis distinguishes between artificial reef and non-reef bacterial taxa. The diagram shows taxa (genus level) with logarithmic LDA scores over 4.0. Nonmetric multidimensional scaling (NMDS) was used to analyze the community composition variations. The results showed that NR samples were significantly separated from the other two clusters (ANOSIM,  $p = 0.003$ ; stress = 0.10), whereas the distribution of TR and CR samples showed no significant difference (Figure 5).

### 3.3. Relationships between Sediment Microbial Communities and Environmental Factors

We can explain the relationship between environmental factors and sediment microbes using redundancy analysis (RDA) by demonstrating the effects of different factors on sediment microbial communities (Figure 6). Based on the model, the top two axes for the sediment bacteria at the genera level could explain 36.07% of the total variance. In the sediment, the concentration of SRP ( $R^2 = 0.59$ ,  $p = 0.032$ ) and TP ( $R^2 = 0.55$ ,  $p = 0.037$ ) were significantly correlated with sediment bacteria community. Finally, we generated a Pearson correlation-based heatmap to illustrate the environmental parameters in clusters

and correlate them with the sediment microbial communities (Figure S4). The resulting heatmap showed the top 30 genera relevant to the environment. The 30 prominent genera are clustered into two main branches. The first branch, *Pseudomonas*, *Lactobacillus*, and *Ralstonia*, had a significant positive correlation with SRP, TP,  $\text{NO}_3^-$ , and TN but a negative association with pH, salinity, Hg, and depth. In contrast, the Candidatus *Nitrosopumilus*, *Thalassotalea*, *Photobacterium*, *Vibrio*, and OM182 clade significantly correlated with SRP, TP,  $\text{NO}_3^-$ , and TN, but had a positive correlation with pH, salinity, Hg, and depth.

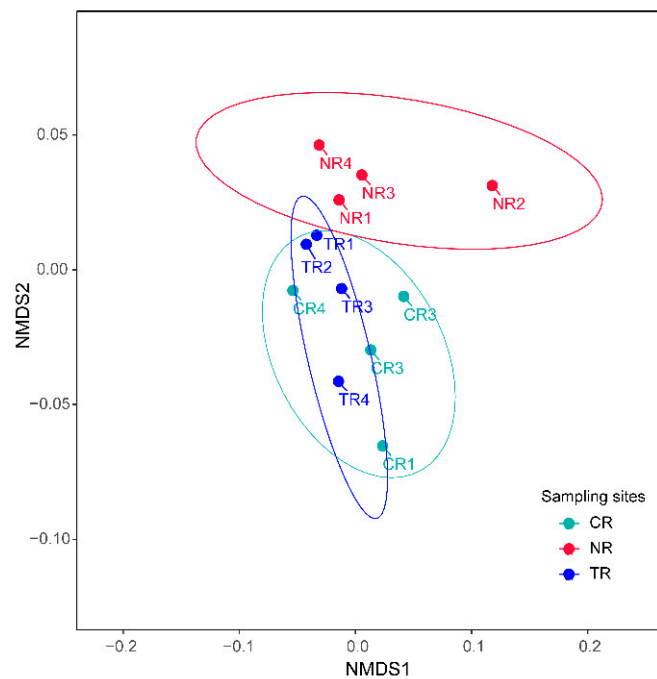


**Figure 5.** Nonmetric multidimensional scaling (NMDS) ordination of sediment bacterial beta-diversities, measured by Bray Curtis dissimilarity between genera relative abundance profiles. The ellipse refers to a 95% confidence interval.

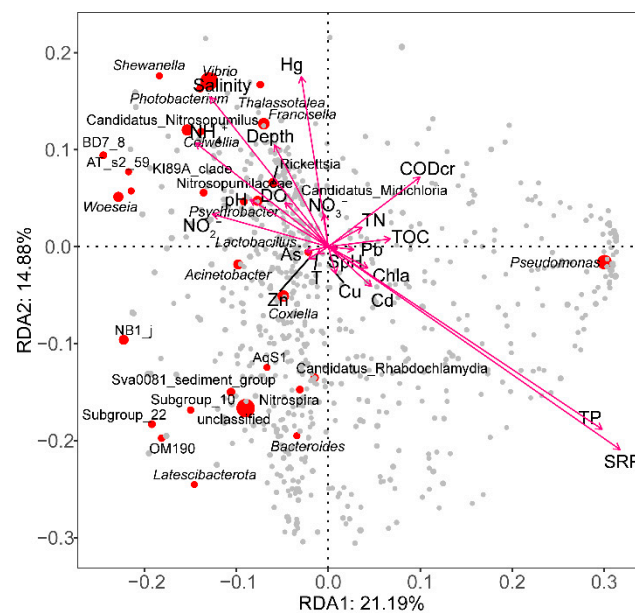


**Figure 6.** Redundancy analysis (RDA) ordination diagram of relative abundance of sediment bacterial genera and environment factors.

### 3.4. Bacterial Relationships within the Sediment Microbial Communities

A correlation network analysis was performed on the co-occurrence of the top 30 abundance microbial genera (Spearman correlation coefficient > 0.4) to find associations between bacteria in the sediment microbial communities (Figure 7). The significant correlations among bacteria found in the sediment samples from three sea areas revealed distinct patterns. The genera that were significantly correlated ( $p < 0.05$ ) with other genera and had a relative abundance of > 1% were selected as keystone taxa [16]. There were 38 significant positive correlation nodes in NR and 52 significant negative correlation nodes. In contrast, the correlation network contained nine phyla. Potential keystone taxa in the NR sediment network include five genera affiliated with two phyla such as *Vibrio*, *Francisella*, *Acinetobacter*, *Rickettsia*, and NB1-j. Furthermore, *Vibrio* and *Francisella* served as network module hubs, and members from phylum Proteobacteria served as module hubs and connectors. TR had 44 significant positive correlation nodes and 40 negative correlation nodes. The correlation network contained 12 phyla. Four genera affiliated with three phyla, including *Vibrio*, *Woeseia*, *Lactobacillus*, and Subgroup-22, were identified as potential keystone taxa in the TR sediment network. Moreover, *Vibrio* served as the module hubs in the network, and members from phylum Proteobacteria served as module hubs and connectors.

CR had more significant positive correlation nodes than NR and TR, with 64 significant positive and 22 negative correlation nodes. The correlation network contained 11 phyla. Nine genera affiliated with three phyla, including *Pseudomonas*, *Vibrio*, *Coxiella*, *Francisella*, *Candidatus Nitrosopumilus*, NB1-j, *Candidatus Midichloria*, Sva0081 sediment group, and *Acinetobacter* were identified as potential keystone taxa in CR sediment network. In addition, *Pseudomonas*, *Vibrio*, and *Coxiella* served as the module hubs in the network, and members from the phylum Proteobacteria served as the module hubs and connectors.

### 3.5. Sediment Microbial Functional Annotation

The FAPROTAX model predicted 59 functions for the ASVs in the sediment samples. Chemoheterotrophy was the predominant function (14.45% of total relative abundance) across all samples, followed by aerobic chemoheterotrophy and fermentation. When compared to TR sites, NR sites had a significantly lower relative abundance of ASVs associated with cellulolysis (Kruskal–Wallis,  $p = 0.019$ ) and intracellular parasites ( $p = 0.008$ ). CR sites had a significantly higher representation of groups involved in dark hydrogen oxidation/nitrification than TR ( $p = 0.049$ ) and NR sites ( $p = 0.009$ ). However, the CR sites were significantly lower than NR ( $p = 0.011$ ), associated with fermentation (Table S3).

The relationship between the FAPROTAX function and environmental factors was depicted using a heatmap showing Spearman's rank correlation and  $p$ -value (Figure 8). The top 30 significant FAPROTAX function correlations are clustered into two branches. One branch was primarily positive to the  $\text{NO}_2^-$ , TN, SRP, TP, and TOC but negative to the depth and salinity. In contrast, the other branch was primarily negative to the  $\text{NO}_2^-$ , TN, SRP, TP, and TOC but positive to the depth and salinity. Thiosulfate respiration was the most significant ( $p < 0.05$ ) influenced by the five environmental factors (BST, COD<sub>Cr</sub>,  $\text{NO}_2^-$ , SRP, and TP).

Following that, four environmental factors significantly ( $p < 0.05$ ) affected methanogenesis by reduction of methyl compounds with  $\text{H}_2$ , fermentation, aromatic compound degradation, and nitrate reduction. On the other hand, ten sediment bacteria community functions were significantly ( $p < 0.05$ ) correlated with SRP and TP concentration. Furthermore, depth and pH had a significant ( $p < 0.05$ ) effect on the six sediment bacteria community functions.



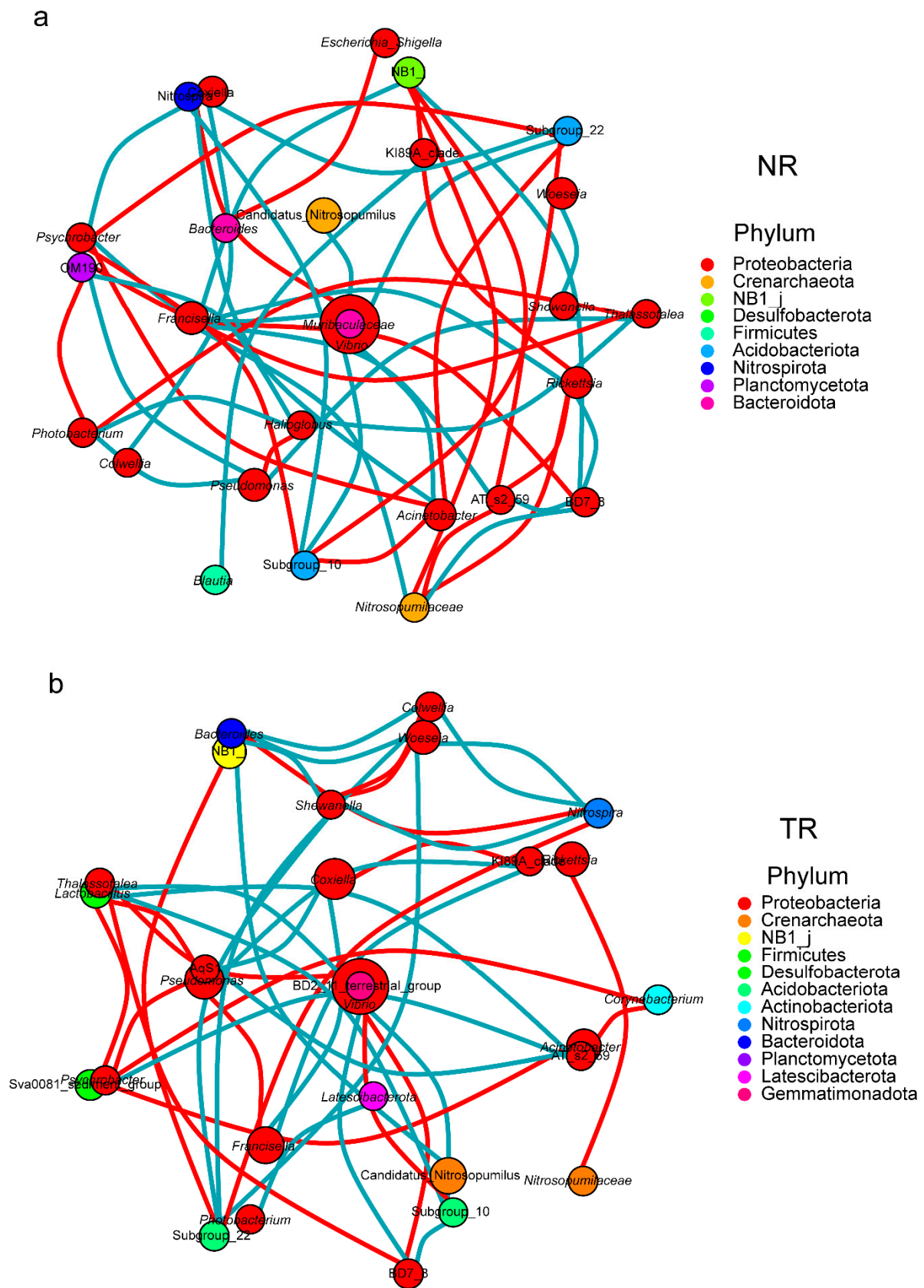
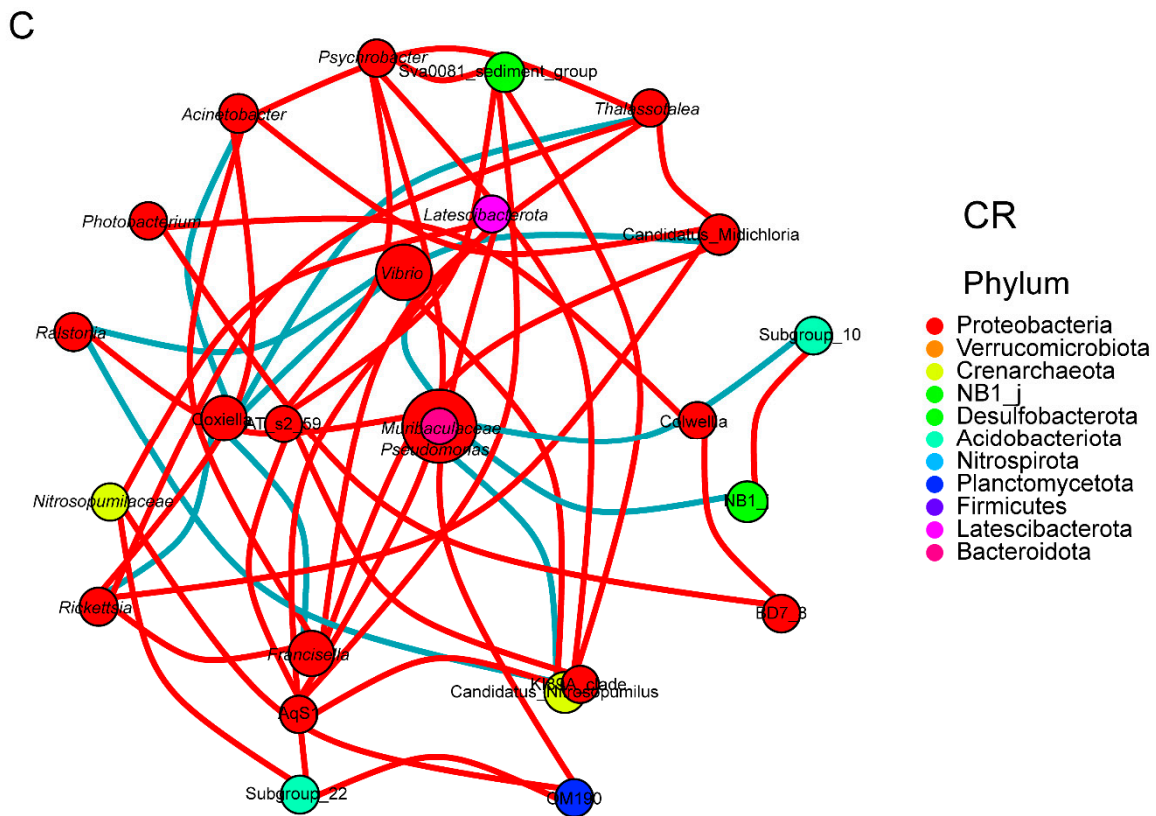
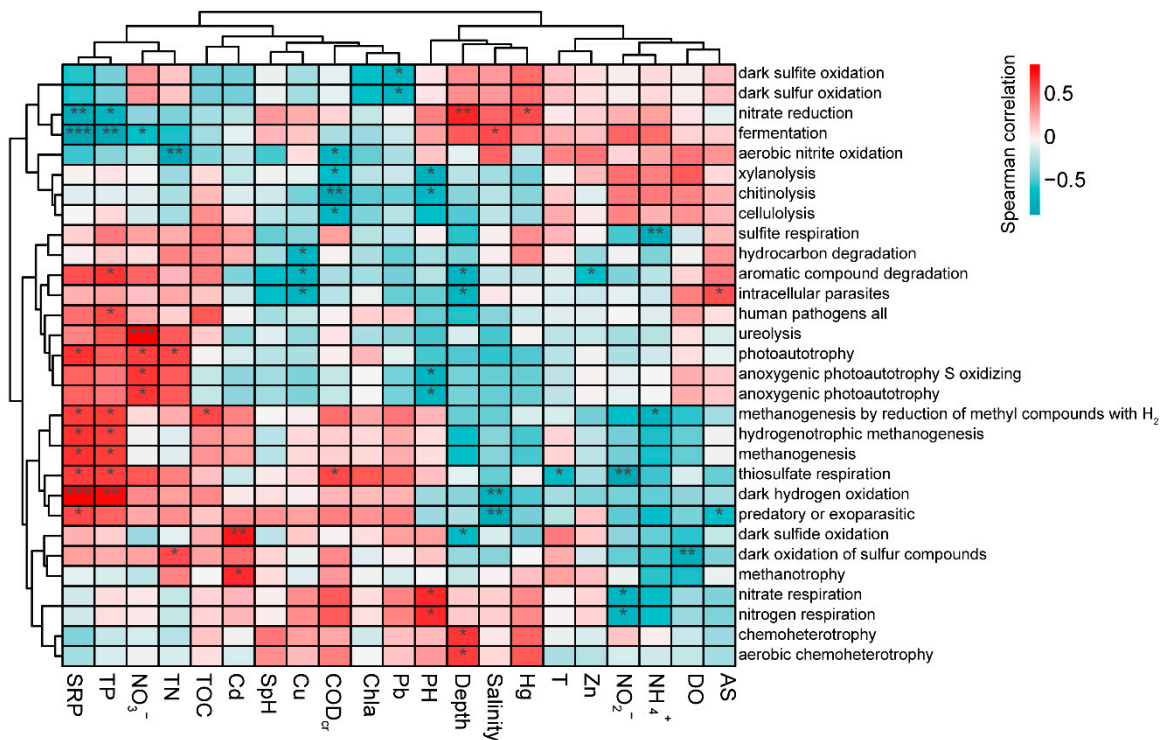


Figure 7. Cont.



**Figure 7.** Correlation network analysis of sediment bacterial genera relative abundance in three areas. (a): NR, (b): TR, (c): CR.



**Figure 8.** Correlation heatmap of bacterial function and environmental factors in the FAPROTAX database for different areas. Different colors indicate the correlation between the environmental factors and potential biogeochemical function predicted by FAPROTAX. \*  $p < 0.05$ , \*\*  $p < 0.01$ , \*\*\*  $p < 0.001$ .

## 4. Discussion

The loss of fishery habitat is one of the important ecological threats faced by the South China Sea [39,40]. China has built large-scale marine ranching to restore the habitat of important fishery waters [2,41]. The previously reported primarily focuses on the impact of marine ranching on fishery resources [42–44]. However, there have been few studies on the long-term changes of microecological communities in the sediments of marine pasture habitats. The present study analyzed the microecological changes of sediments in the artificial reef area and the reef-free control area for ten years and one year and found that the reef throwing behavior was significantly correlated with the local colony characteristics of sediments. The changes in these microbial communities may impact the local environmental characteristics, affecting the ecosystem cycle of local fishery habitats.

### 4.1. Changes in Physicochemical Characteristics of Overlying Water and Sediment

The finding that the pH of overlying water in NR areas was significantly higher than in CR and TR areas may be due to the decomposition of calcium silicate hydrate and calcium hydroxide and decarbonation of  $\text{CaCO}_3$  in the new concrete ARs [45]. This result was consistent with data obtained from the high pH surface region of the new artificial reef [46]. However, the findings of the present study show lower pH of the sediments in TR sites. The overlying water column represents a short-term impact, while the long-term is represented by sediment [16].

The marine biology stocks in the areas around ARs can generally be restored or strengthened after their deployment due to the improved productivity in the region and the accumulation of fish attracted from adjacent areas [47]. The long-term biological deposition causes an increase in humic acid and sulfide in sediments, affecting the sediments' pH [48–51]. Compared to water samples, this emphasizes the sediment samples' accumulation properties and relative stability [52]. Heavy metals are another hot research topic that can easily lead to accumulation. They are persistent, bioaccumulative, and difficult to decompose. The amplification and enrichment of the food chain may cause irreversible damage to the ecological balance and human health [53]. A micro-food loop has been proposed to affirm the importance of marine bacteria in marine ecosystems. Bacteria play an important role in the biological cycle of heavy metals. They are highly efficient microorganisms capable of converting heavy metals into low or nontoxic forms. Several studies are currently being conducted on the bacteria related to heavy metals in marine sediment structures [54]. Biochar can significantly improve heavy metals adsorption capacity. Biochar can fix heavy metals through direct electrostatic attraction, complexation, ion exchange, and precipitation [55]. However, this finding has not previously been described. Although the TOC ranges in the three survey sites were similar, the As of the sediments in CR was significantly lower than in TR. One possible explanation is that ARs contain iron sulphide minerals. It can incorporate trace amounts of arsenic in its structure [56].

Arsenic may release into the environment over time. This is consistent with previous findings, which revealed an excellent linear relationship between Fe/Mn and arsenic content [55,57]. Furthermore, the present study's findings show that the Cu of the sediments in NR was significantly higher than TR. The new ARs induce more Fe,  $\text{CO}_3^{2-}$  and  $\text{OH}^-$ . Cu is easily chemisorbed on or incorporated into a variety of minerals such as chalcopyrite ( $\text{CuFeS}_2$ ), covellite ( $\text{CuS}$ ), and malachite  $\text{Cu}_2\text{CO}_3(\text{OH})_2$ . They remain stable in an alkaline environment [56]. This finding is consistent with the previously described high pH in NR sites.

### 4.2. Sediment Bacterial Community Composition

The present study investigated the abundance and diversity of microbial communities in marine ranching sediments over time, providing a new perspective on the impact of marine pastures on coastal sedimentary habitats. Proteobacteria and Gammaproteobacteria were the most abundant phyla and classes in this study. The finding is consistent with that of

Zhuang [58], who determined microbial community structure in Eastern Guangdong shore sediment. However, the following phyla differed from those previously described [58,59].

It is worth noting that Pielou's evenness and Shannon index of NR were significantly lower than those of CR and TR ( $p < 0.05$ ). Compared with TR or CR sediments, the NR area exhibits a distinct pattern of bacterial diversity. The findings of the present study suggest that the newly formed ARs may have influenced the indigenous sediment microbial community structure. The results are consistent with previous studies [6,16,51]. However, as time passes, the impact of the reef on the microbial community structure of sediments will diminish. Finally, there was no statistically significant difference in the CR area. Not only the alpha diversity presented the above differences, but also the beta diversity results showed similar trends between the study areas through the NMDS. This could result from long-term microbial communities' succession in the TR area [6].

The biomarkers were considered part of the core microorganisms [60]. The LEfSe analysis revealed that Alphaproteobacteria (class level), Moraxellaceae (family level), *Acinetobacter*, Rickettsiales (order level), and Candidatus Midichloria (genus level) of phylum Proteobacteria enriched TR sediment. The wide distribution of Alphaproteobacteria in sediment environments has been well documented [52]. Previous studies have highlighted the importance of Alphaproteobacteria. They are important in decomposing and assimilating organic matter in organically enriched sediments [61]. The increase of Alphaproteobacteria could be attributed to the addition of organic matter in TR sediment [62]. Moraxellaceae was closely related to seawater salinity, making it a potential indicator of seawater invasion [63]. Similarly, *Acinetobacter* occupies an important position in sediment because it is ubiquitous. The multifunctional metabolic characteristics enable it to catabolize various natural compounds. It actively participates in the nutrient cycle of the sediment ecosystem [64]. Candidatus Midichloria and Rickettsiales are ecologically widespread intracellular symbionts found in the sediment. They were infected with aquatic protozoa [65,66].

In comparison to the TR, NR biomarkers were simple. *Francisella* are new bacteria with high virulence that can kill a large number of tilapia. These bacteria also affect many other fishes, including hybrid striped bass and various ornamental fishes [67]. The finding is also consistent with previous observations, which revealed a high abundance of *Francisella* in sediments and water [68,69]. Ulteriorly, these findings also support previous research indicating that Lactobacillales could be used as potential biomarkers in the Nile water [52]. Interestingly, some of the biomarkers are taxa known for their pathogenic potential, such as *Coxiella*, Lactobacillales, and Bacilli [70].

Although we cannot generalize about all species belonging to a particular genus, they have been associated with certain diseases [71]. On the other hand, Bacilli and Lactobacillales of phylum Firmicutes were widely distributed in the sediment and intestinal content. These organisms were typically anaerobic and chemoorganotrophic [72]. They could be identified as potential biomarkers in the CR sediment.

#### 4.3. Relationships between Sediment Microbial Communities and Environmental Factors

RDA correlates microbiota distribution variability to environmental variables. The SRP and TP concentration was thought to be the main driving force in shaping the microbial community in the sediment. These results seem to be consistent with previous research that found that sediment chemical components (i.e., nitrogen and phosphorus concentrations) regulate and form the diversity of bacterial communities [73,74]. The sedimentation environment has shaped different microorganisms, and microorganisms have influenced their habitat environment [12]. Furthermore, the Pearson correlation-based results indicate that *Pseudomonas*, *Lactobacillus*, and *Ralstonia* had a significant positive correlation with SRP, TP,  $\text{NO}_3^-$ , and TN, but a negative association with pH, salinity, Hg, and depth. These results are in line with previous studies. *Pseudomonas* has been isolated from both aquatic and terrestrial ecosystems worldwide. It usually has ecologically important characteristics, including the potential of denitrification and the ability to degrade xenobiotics [75]. It is

worth noting that *Pseudomonas* and *Ralstonia* have a high capacity for removing Pb and Hg from marine sediment [76,77]. The relative abundance of *Pseudomonas* and *Ralstonia* was significantly higher in CR. Consequently, the CR was better suited to their survival. The present study suggests that this area of sediment microbial communities may be subjected to heavy metal stress. However, the *Photobacterium*, *Vibrio*, and *Thalassotalea* had a significant negative correlation with SRP, TP,  $\text{NO}_3^-$ , and TN, but a positive association with pH, salinity, Hg, and depth. *Photobacterium*, *Vibrio*, and *Thalassotalea* commonly occur in seawater and cooperate with marine animals. Some are highly specific bioluminescent mutualisms with marine fish and squid [78,79]. These genera were found to have a higher relative abundance in NR. These findings indicated that these bacteria are preferentially inhabited in NR in abiotic conditions (lower SRP, TP,  $\text{NO}_3^-$  and TN, but higher pH and salinity) and biotic conditions (developing fishery resources).

#### 4.4. Bacterial Relationships within the Sediment Microbial Communities

The correlation network analysis revealed the structure and interactions of the microbial communities in sediment. In the present study, we analyzed the co-occurrence patterns of bacterial communities in the old and new marine ranching at genus levels. We identified the keystone taxa using topological parameters of network analysis. The significant differences in the structures of the correlation networks between areas were explored, indicating that marine ranching significantly impacted the correlation networks of the microorganisms in the sediment [80]. According to the current correlation network results in CR, this is consistent with the fact that microbes from the same domain frequently had significant and predominantly positive correlations with each other [81]. This could imply that mature and stable microbial communities exist in CR. Surprisingly, NR was found to have more negative correlation nodes, indicating that taxa face more competition or predation pressure [82]. However, as time passes, the negative relationship between micro-ecosystem deposition has weakened in TR. These results suggested that after being subjected to disturbance and succession [83], the sediment bacteria community gradually adapted to the existing conditions and reached a relatively stable state.

Compared to other taxa in the network, keystone taxa play an important role in maintaining the network structure of the sediment bacteria community [81]. Some keystones can act as transporters, regulators, and module hubs in bacterial communities, which are critical to the overall stability of the entire microbial network structure [84]. Surprisingly, *Vibrio* served as the module-hubs in the network in all areas. These findings indicate that marine ranching constructions had little influence. *Vibrio* is a typical heterogeneous bacterium widely distributed in marine ecosystems and is usually associated with a high nutritional environment. They are thought to be a potential indicator of eutrophication. In addition, previous studies have shown that *Vibrio* has a variety of metabolic capabilities, including nitrogen fixation, phosphate compound intake, organic matter utilization, and remineralization [19].

Moreover, some pathogenic bacteria from this genus may infect humans and aquaculture [85]. Another possible explanation for the enrichment of *Vibrio* was the high-density mariculture of coastal waters [86]. Our findings align with previous research indicating that *Vibrio* may be dominant in high disturbance areas [38]. Collectively, the current results suggest such keystone taxa should be given more attention.

#### 4.5. Sediment Microbial Functional Annotation

FAPROTAX was used to evaluate the potential functional differences between marine ranching stages and the control area. The present study showed that chemoheterotrophy, aerobic chemoheterotrophy, and fermentation were the top three main functions of the three areas that account for 59.96% relative abundance of the functional annotation. These results are consistent with findings from other marine microcosms [87–89]. However, when we focused on more specific functions, we found that the dominant functions involved in biogeochemical cycling differed depending on the sediment microbial ecosystem. It

was found that only the fermentation of the three primary functions differed significantly among areas. Fermentation was significantly higher in NR sites compared to CR. This disparity could be attributed to extra organic matter deposition by the increased biomass in NR [90]. On the other hand, the cellulolysis and intracellular parasite function were higher in TR than in NR. This result could be explained by the fact that TR's macroalgae and reef creature biomass were higher [91].

As environmental factors influence bacterial communities, the potential functions are consistent with the changes in environmental factors, particularly energy sources, the phosphorus cycle, and inorganic nitrogen [87]. In the current study, the heatmap between FAPROTAX function and environmental factors also revealed that  $\text{NO}_2^-$ , TN, SRP, TP, TOC, depth, and salinity were the key driving factors of the potential biogeochemical functions in the sediment. The key driving factors are consistent with previous research on the relationships between sediment microbial communities and environmental factors. Therefore, the impact of different bacteria in sediments could alter the amount of biogeochemical cycle in the marine ranching ecosystem [92]. In the marine ranching ecosystem, sedimentary colonies may play an important role in nutrient and carbon cycling, interacting with other organisms [81]. In addition, ARs affect the water flow field and accelerate the change of mineral composition of sediments that may support the electrical coupling of more complex microbial redox reactions, contributing to biogeochemical cycling and maintaining ecological stability [47,93,94].

## 5. Conclusions

Overall, the present study provided a more in-depth understanding of sediment microbial communities in marine ranching. Artificial reefs significantly impact these geochemical parameters (i.e.,  $\text{NO}_3^-$ , TN, SRP, TP, and pH). Meanwhile, nutrient concentrations and pH are the primary factors influencing the compositions and structure of the bacterial community in the sediments of an artificial reef. The new artificial reefs reduced sediment alpha diversity. The significant net correlations among bacteria identified in sediment samples from three sea areas showed different patterns. The distribution of potential biogeochemical functions concerning carbon and nutrient cycles in bacterial communities was strongly influenced by sediment environmental conditions, especially  $\text{NO}_2^-$ , TN, SRP, TP, TOC, depth, and salinity. This may impact the trophic transfer of energy in marine ranching food webs. These findings provided new perspectives for investigating the effects of artificial reef disturbances on sediment microbes and facilitated sedimental environment monitoring based on microbial community composition.

**Supplementary Materials:** The following supporting information can be downloaded at: <https://www.mdpi.com/article/10.3390/su142214728/s1>, Figure S1. Shannon rarefaction curve; Figure S2. Taxonomic profile of bacterial communities of sediment samples in phylum level. Only the top 20 relative abundance phyla were shown; Figure S3. Ternary plots of the genera and phyla for bacteria in three sea areas sediment; Figure S4. Pearson correlation-based heatmap of the environment factors and sediment microbial communities from sediment samples; Table S1. the geochemical characteristics of overlying water and sediment among different areas; Table S2. Kruskal-Wallis with Dunn's multiple-comparisons test of Physicochemical characteristics of the overlying water and sediment samples between sampling sites; Table S3. Kruskal-Wallis with Dunn's multiple-comparisons test of FAPROTAX model predicted between sampling sites.

**Author Contributions:** F.T.: Writing original draft, Conceptualization, Methodology, Software, Validation; G.C.: Visualization; X.F.: Formal analysis, Resources, Data curation; Y.L.: Investigation; P.C.: Review & editing Conceptualization, Supervision. All authors have read and agreed to the published version of the manuscript.

**Funding:** This work was supported by Key-Area Research and Development Program of Guangdong (2020B1111030002-2), Shenzhen Science and Technology Innovation Project (JCYJ20160331141759795) and Zhuhai Fishery Resources Background Survey Project (GX20143FW).

**Institutional Review Board Statement:** All experiments were performed under the approval of the Ethics Committee of South China Sea Fisheries Research Institute, Chinese Academy of Fishery Sciences.

**Informed Consent Statement:** Not applicable.

**Data Availability Statement:** The raw sequence data are available in the National Center for Biotechnology Information (NCBI, Bethesda, MD, USA). All sequencing data are stored in the PRJNA880993 biological project.

**Acknowledgments:** The authors are grateful to Zhijian Chen and Jianhao Zhou for their assistance with investigation and sample collection.

**Conflicts of Interest:** The authors declare that they have no known any commercial or financial relationships that could be appeared as a potential conflict of interest.

## References

1. Qin, M.; Yue, C.; Du, Y. Evolution of China's marine ranching policy based on the perspective of policy tools. *Mar. Policy* **2020**, *117*, 103941. [\[CrossRef\]](#)
2. Yu, J.; Zhang, L. Evolution of marine ranching policies in China: Review, performance and prospects. *Sci. Total Environ.* **2020**, *737*, 139782. [\[CrossRef\]](#)
3. Qin, M.; Wang, X.; Du, Y.; Wan, X. Influencing factors of spatial variation of national marine ranching in China. *Ocean Coast. Manag.* **2021**, *199*, 105407. [\[CrossRef\]](#)
4. Wang, Y.; Guo, T.; Cheng, T.C.E.; Wang, N. Evolution of blue carbon trading of China's marine ranching under the blue carbon special subsidy mechanism. *Ocean Coast. Manag.* **2022**, *222*, 106123. [\[CrossRef\]](#)
5. Tan, Y.; Lou, S. Research and development of a large-scale modern recreational fishery marine ranch System. *Ocean Eng.* **2021**, *233*, 108610. [\[CrossRef\]](#)
6. Guo, Z.; Wang, L.; Cong, W.; Jiang, Z.; Liang, Z. Comparative analysis of the ecological succession of microbial communities on two artificial reef materials. *Microorganisms* **2021**, *9*, 120. [\[CrossRef\]](#) [\[PubMed\]](#)
7. Nie, Z.; Zhu, L.; Xie, W.; Zhang, J.; Wang, J.; Jiang, Z.; Liang, Z. Research on the influence of cut-opening factors on flow field effect of artificial reef. *Ocean Eng.* **2022**, *249*, 110890. [\[CrossRef\]](#)
8. Jiang, Z.; Liang, Z.; Zhu, L.; Liu, Y. Numerical simulation of effect of guide plate on flow field of artificial reef. *Ocean Eng.* **2016**, *116*, 236–241. [\[CrossRef\]](#)
9. Neumann, C.; Faria, E.F.; Dos Santos, A.C.P. Concrete leaching of a hydroelectric powerhouse due to 40 years of exposure to river water. *Constr. Build. Mater.* **2021**, *302*, 124253. [\[CrossRef\]](#)
10. Yi, Y.; Zhu, D.; Guo, S.; Zhang, Z.; Shi, C. A review on the deterioration and approaches to enhance the durability of concrete in the marine environment. *Cem. Concr. Compos.* **2020**, *113*, 103695. [\[CrossRef\]](#)
11. Zhang, D.; Li, M.; Yang, Y.; Yu, H.; Xiao, F.; Mao, C.; Huang, J.; Yu, Y.; Wang, Y.; Wu, B.; et al. Nitrite and nitrate reduction drive sediment microbial nitrogen cycling in a eutrophic lake. *Water Res.* **2022**, *220*, 118637. [\[CrossRef\]](#) [\[PubMed\]](#)
12. Pierangeli, G.M.F.; Domingues, M.R.; Choueri, R.B.; Hanisch, W.S.; Gregoracci, G.B.; Benassi, R.F. Spatial variation and environmental parameters affecting the abundant and rare communities of bacteria and archaea in the sediments of tropical urban reservoirs. *Microb. Ecol.* **2022**, *83*, 2047. [\[CrossRef\]](#)
13. Dong, X.; Zhang, C.; Li, W.; Weng, S.; Song, W.; Li, J.; Wang, Y. Functional diversity of microbial communities in inactive seafloor sulfide deposits. *FEMS Microbiol. Ecol.* **2021**, *97*, b108. [\[CrossRef\]](#)
14. Roberto, A.A.; Van Gray, J.B.; Leff, L.G. Sediment bacteria in an urban stream: Spatiotemporal patterns in community composition. *Water Res.* **2018**, *134*, 353–369. [\[CrossRef\]](#) [\[PubMed\]](#)
15. Shi, R.; Han, T.; Huang, H.; Kuang, Z.; Qi, Z. The extent and pattern of mariculture impacts on spatial and seasonal variations of sediment bacterial communities among three coastal waters. *Front. Mar. Sci.* **2022**, *9*, 782456. [\[CrossRef\]](#)
16. Fang, G.; Yu, H.; Sheng, H.; Tang, Y.; Liang, Z. Comparative analysis of microbial communities between water and sediment in Laoshan Bay marine ranching with varied aquaculture activities. *Mar. Pollut. Bull.* **2021**, *173*, 112990. [\[CrossRef\]](#)
17. Vila-Costa, M.; Cerro-Gálvez, E.; Martínez-Varela, A.; Casas, G.; Dachs, J. Anthropogenic dissolved organic carbon and marine microbiomes. *ISME J.* **2020**, *14*, 2646–2648. [\[CrossRef\]](#)
18. Kumar Parida, P.; Behera, B.K.; Dehury, B.; Rout, A.K.; Sarkar, D.J.; Rai, A.; Das, B.K.; Mohapatra, T. Community structure and function of microbiomes in polluted stretches of river Yamuna in New Delhi, India, using shotgun metagenomics. *Environ. Sci. Pollut. R.* **2022**, *29*, 1–15. [\[CrossRef\]](#)
19. Li, N.; Dong, K.; Jiang, G.; Tang, J.; Xu, Q.; Li, X.; Kang, Z.; Zou, S.; Chen, X.; Adams, J.M.; et al. Stochastic processes dominate marine free-living *Vibrio* community assembly in a subtropical gulf. *FEMS Microbiol. Ecol.* **2020**, *96*, a198. [\[CrossRef\]](#)
20. Lao, Q.; Su, Q.; Liu, G.; Shen, Y.; Chen, F.; Lei, X.; Qing, S.; Wei, C.; Zhang, C.; Gao, J. Spatial distribution of and historical changes in heavy metals in the surface seawater and sediments of the Beibu Gulf, China. *Mar. Pollut. Bull.* **2019**, *146*, 427–434. [\[CrossRef\]](#)
21. Yao, Y.; Wang, C. Variations in Summer Marine Heatwaves in the South China Sea. *J. Geophys. Res. Ocean.* **2021**, *126*, e2021J–e17792. [\[CrossRef\]](#)

22. Hampel, J.J.; Moseley, R.D.; Hamdan, L.J. Microbiomes respond predictably to built habitats on the seafloor. *Mol. Ecol.* **2022**. [[CrossRef](#)]
23. Zhou, Z.; Meng, H.; Gu, W.; Li, J.; Deng, M.; Gu, J. High-throughput sequencing reveals the main drivers of niche-differentiation of bacterial community in the surface sediments of the northern South China sea. *Mar. Environ. Res.* **2022**, *178*, 105641. [[CrossRef](#)] [[PubMed](#)]
24. Zhang, H.; Huang, T.; Chen, S.; Yang, X.; Lv, K.; Sekar, R. Abundance and diversity of bacteria in oxygen minimum drinking water reservoir sediments studied by quantitative PCR and pyrosequencing. *Microb. Ecol.* **2015**, *69*, 618–629. [[CrossRef](#)] [[PubMed](#)]
25. Duan, L.; Li, J.; Yin, L.; Luo, X.; Ahmad, M.; Fang, B.; Li, S.; Deng, Q.; Wang, P.; Li, W. Habitat-dependent prokaryotic microbial community, potential keystone species, and network complexity in a subtropical estuary. *Environ. Res.* **2022**, *212*, 113376. [[CrossRef](#)]
26. Chen, Q.; Chen, P. Changes in the heavy metals and petroleum hydrocarbon contents in seawater and surface sediment in the year following artificial reef construction in the Pearl River Estuary, China. *Environ. Sci. Pollut. Res.* **2020**, *27*, 6009–6021. [[CrossRef](#)]
27. Oh, S.; Shin, W.S.; Kim, H.T. Effects of pH, dissolved organic matter, and salinity on ibuprofen sorption on sediment. *Environ. Sci. Pollut. Res. Int.* **2016**, *23*, 22882–22889. [[CrossRef](#)]
28. Rajeev, M.; Sushmitha, T.J.; Toleti, S.R.; Pandian, S.K. Sediment-associated bacterial community and predictive functionalities are influenced by choice of 16S ribosomal RNA hypervariable region(s): An amplicon-based diversity study. *Genomics* **2020**, *112*, 4968–4979. [[CrossRef](#)]
29. Hamdan, H.Z.; Salam, D.A. Microbial community evolution during the aerobic biodegradation of petroleum hydrocarbons in marine sediment microcosms: Effect of biostimulation and seasonal variations. *Environ. Pollut.* **2020**, *265*, 114858. [[CrossRef](#)]
30. Callahan, B.J.; Mcmurdie, P.J.; Rosen, M.J.; Han, A.W.; Johnson, A.J.A.; Holmes, S.P. DADA2: High-resolution sample inference from Illumina amplicon data. *Nat. Methods* **2016**, *13*, 581–583. [[CrossRef](#)]
31. Bokulich, N.A.; Kaehler, B.D.; Rideout, J.R.; Dillon, M.; Bolyen, E.; Knight, R.; Huttley, G.A.; Gregory Caporaso, J. Optimizing taxonomic classification of marker-gene amplicon sequences with QIIME 2's q2-feature-classifier plugin. *Microbiome* **2018**, *6*, 90. [[CrossRef](#)] [[PubMed](#)]
32. Lastauskien, E.; Valskys, V.; Stankeviiūt, J.; Kalcien, V.; Armalyt, J. The impact of intensive fish farming on pond sediment microbiome and antibiotic resistance gene composition. *Front. Vet. Sci.* **2021**, *8*, 673756. [[CrossRef](#)]
33. Love, M.I.; Huber, W.; Anders, S. Moderated estimation of fold change and dispersion for RNA-seq data with DESeq2. *Genome Biology* **2014**, *15*, 550. [[CrossRef](#)] [[PubMed](#)]
34. Mandal, S.; Van Treuren, W.; White, R.A.; Eggesbø, M.; Knight, R.; Peddada, S.D. Analysis of composition of microbiomes: A novel method for studying microbial composition. *Microb. Ecol. Health Dis.* **2015**, *26*, 27663. [[CrossRef](#)]
35. Vázquez-Baeza, Y.; Pirrung, M.; Gonzalez, A.; Knight, R. EMPeror: A tool for visualizing high-throughput microbial community data. *GigaScience* **2013**, *2*, 16. [[CrossRef](#)] [[PubMed](#)]
36. Oksanen, J.; Blanchet, F.G.; Friendly, M.; Kindt, R.; Wagner, H.H. Vegan Community Ecology Package Version 2.5. 2020. Available online: <https://cran.r-project.org/web/packages/BiodiversityR/index.html> (accessed on 7 November 2020).
37. Langille, M.G.I.; Zaneveld, J.; Caporaso, J.G.; McDonald, D.; Knights, D.; Reyes, J.A.; Clemente, J.C.; Burkepile, D.E.; Vega Thurber, R.L.; Knight, R.; et al. Predictive functional profiling of microbial communities using 16S rRNA marker gene sequences. *Nat. Biotechnol.* **2013**, *31*, 814–821. [[CrossRef](#)] [[PubMed](#)]
38. Long, Y.; Jiang, J.; Hu, X.; Hu, J.; Ren, C.; Zhou, S. The response of microbial community structure and sediment properties to anthropogenic activities in Caohai wetland sediments. *Ecotox. Environ. Safe.* **2021**, *211*, 111936. [[CrossRef](#)]
39. Zhou, X.; Zhao, X.; Zhang, S.; Lin, J. Marine ranching construction and management in east china sea: Programs for sustainable fishery and aquaculture. *Water-Sui.* **2019**, *11*, 1237. [[CrossRef](#)]
40. Wang, Y.; Yao, L.; Chen, P.; Yu, J.; Wu, Q.E. Environmental influence on the spatiotemporal variability of fishing grounds in the Beibu Gulf, South China Sea. *J. Mar. Sci. Eng.* **2020**, *8*, 957. [[CrossRef](#)]
41. Liu, S.; Zhou, X.; Zeng, C.; Frankstone, T.; Cao, L. Characterizing the development of Sea ranching in China. *Rev. Fish Biol. Fisher.* **2022**, *32*, 783–803. [[CrossRef](#)]
42. Wang, Y.; Zhang, W. Maximum sustainable yield estimation of enhancement species with the characteristics of movement inside and outside marine ranching. *J. Oceanol. Limnol.* **2021**, *39*, 2380–2387. [[CrossRef](#)]
43. Yanfeng, W.; Qiwei, H.U.; Jing, Y.U.; Pimao, C.; Liming, S. Effect assessment of fishery resources proliferation in Zhelin Bay marine ranching in eastern Guangdong. *South China Fish. Sci.* **2019**, *15*, 12. [[CrossRef](#)]
44. Li, J.; Yin, Z.; Yang, J.; Chen, L.; Xu, M.; Zhang, Y.; Wu, Z.; Tian, T. Analysis of spring community structure and evaluation of ecological niche in tangshan marine ranching, China. *Sustainability* **2022**, *14*, 6999. [[CrossRef](#)]
45. Uthaman, S.; Vishwakarma, V.; George, R.P.; Ramachandran, D.; Kumari, K.; Preetha, R.; Premila, M.; Rajaraman, R.; Mudali, U.K.; Amarendra, G. Enhancement of strength and durability of fly ash concrete in seawater environments: Synergistic effect of nanoparticles. *Constr. Build. Mater.* **2018**, *187*, 448–459. [[CrossRef](#)]
46. Xu, Q.; Ji, T.; Yang, Z.; Ye, Y. Preliminary investigation of artificial reef concrete with sulphoaluminate cement, marine sand and sea water. *Constr. Build. Mater.* **2019**, *211*, 837–846. [[CrossRef](#)]
47. Song, M.; Wang, J.; Nie, Z.; Wang, L.; Wang, J.; Zhang, J.; Wang, Y.; Guo, Z.; Jiang, Z.; Liang, Z. Evaluation of artificial reef habitats as reconstruction or enhancement tools of benthic fish communities in northern Yellow Sea. *Mar. Pollut. Bull.* **2022**, *182*, 113968. [[CrossRef](#)]



48. Wang, L.; Liang, Z.; Guo, Z.; Cong, W.; Song, M.; Wang, Y.; Jiang, Z. Response mechanism of microbial community to seasonal hypoxia in marine ranching. *Sci. Total Environ.* **2022**, *811*, 152387. [[CrossRef](#)]
49. White, C.A.; Nichols, P.D.; Ross, D.J.; Dempster, T. Dispersal and assimilation of an aquaculture waste subsidy in a low productivity coastal environment. *Mar. Pollut. Bull.* **2017**, *120*, 309–321. [[CrossRef](#)]
50. Zlatkovic, S. Some metabolic, diversity and toxicity aspects of bacterial communities life in aquatic sediments. *MedCrave Online* **2017**, *5*, 156. [[CrossRef](#)]
51. Wang, Y.; Sun, J.; Fang, E.; Guo, B.; Dai, Y.; Gao, Y.; Wang, H.; Zhang, X.; Xu, X.; Yu, Y.; et al. Impact of artificial reefs on sediment bacterial structure and function in Bohai Bay. *Can. J. Microbiol.* **2018**, *65*, 191–200. [[CrossRef](#)]
52. Eraqi, W.A.; Elrakaiby, M.T.; Megahed, S.A.; Yousef, N.H.; Elshahed, M.S.; Yassin, A.S. Spatiotemporal analysis of the water and sediment Nile microbial community along an urban metropolis. *Microb. Ecol.* **2021**, *82*, 288–298. [[CrossRef](#)] [[PubMed](#)]
53. Chen, Y.; Shi, Q.; Qu, J.; He, M.; Liu, Q. A pollution risk assessment and source analysis of heavy metals in sediments: A case study of Lake Gehu, China. *Chinese J. Anal. Chem.* **2022**, *50*, 100077. [[CrossRef](#)]
54. Kalkan, S. Heavy metal resistance of marine bacteria on the sediments of the Black Sea. *Mar. Pollut. Bull.* **2022**, *179*, 113652. [[CrossRef](#)] [[PubMed](#)]
55. Ji, X.; Wan, J.; Wang, X.; Peng, C.; Wang, G.; Liang, W.; Zhang, W. Mixed bacteria-loaded biochar for the immobilization of arsenic, lead, and cadmium in a polluted soil system: Effects and mechanisms. *Sci. Total Environ.* **2022**, *811*, 152112. [[CrossRef](#)] [[PubMed](#)]
56. Thanh-Nho, N.; Marchand, C.; Strady, E.; Vinh, T.; Nhu-Trang, T. Metals geochemistry and ecological risk assessment in a tropical mangrove (Can Gio, Vietnam). *Chemosphere* **2019**, *219*, 365–382. [[CrossRef](#)]
57. Liu, E.; Yang, Y.; Xie, Z.; Wang, J.; Chen, M. Influence of sulfate reduction on arsenic migration and transformation in groundwater environment. *Water* **2022**, *14*, 942. [[CrossRef](#)]
58. Zhuang, M.; Sanganyado, E.; Li, P.; Liu, W. Distribution of microbial communities in metal-contaminated nearshore sediment from Eastern Guangdong, China. *Environ. Pollut.* **2019**, *250*, 482–492. [[CrossRef](#)]
59. Vipindas, P.V.; Mujeeb, R.K.M.; Jabir, T.; Thasneem, T.R.; Mohamed Hatha, A.A. Diversity of sediment bacterial communities in the South Eastern Arabian Sea. *Reg. Stud. Mar. Sci.* **2020**, *35*, 101153. [[CrossRef](#)]
60. Qi, Q.; Hu, C.; Lin, J.; Wang, X.; Tang, C.; Dai, Z.; Xu, J. Contamination with multiple heavy metals decreases microbial diversity and favors generalists as the keystones in microbial occurrence networks. *Environ. Pollut.* **2022**, *306*, 119406. [[CrossRef](#)]
61. Wang, Z.; Yang, Y.; Sun, W.; Xie, S. Biodegradation of nonylphenol by two alphaproteobacterial strains in liquid culture and sediment microcosm. *Int. Biodeter. Biodegr.* **2014**, *92*, 1–5. [[CrossRef](#)]
62. Kunihiro, T.; Takasu, H.; Miyazaki, T.; Uramoto, Y.; Kinoshita, K.; Yodnarasi, S.; Hama, D.; Wada, M.; Kogure, K.; Ohwada, K.; et al. Increase in Alphaproteobacteria in association with a polychaete, *Capitella* sp. I, in the organically enriched sediment. *ISME J.* **2011**, *5*, 1818–1831. [[CrossRef](#)] [[PubMed](#)]
63. Li, Y.; Huang, D.; Sun, W.; Sun, X.; Yan, G.; Gao, W.; Lin, H. Characterizing sediment bacterial community and identifying the biological indicators in a seawater-freshwater transition zone during the wet and dry seasons. *Environ. Sci. Pollut. R.* **2022**, *29*, 41219–41230. [[CrossRef](#)]
64. Jung, J.; Park, W. *Acinetobacter* species as model microorganisms in environmental microbiology: Current state and perspectives. *Appl. Microbiol. Biot.* **2015**, *99*, 2533–2548. [[CrossRef](#)]
65. Bonthond, G.; Merselis, D.G.; Dougan, K.E.; Graff, T.; Todd, W.; Fourqurean, J.W.; Rodriguez-Lanetty, M. Inter-domain microbial diversity within the coral holobiont *Siderastrea siderea* from two depth habitats. *PeerJ* **2018**, *6*, e4323. [[CrossRef](#)]
66. Montagna, M.; Sasser, D.; Epis, S.; Bazzocchi, C.; Vannini, C.; Lo, N.; Sacchi, L.; Fukatsu, T.; Petroni, G.; Bandi, C. “*Candidatus* Midichloriaceae” fam. nov. (Rickettsiales), an Ecologically Widespread Clade of Intracellular Alphaproteobacteria. *Appl. Environ. Microb.* **2013**, *79*, 3241–3248. [[CrossRef](#)]
67. Poudyal, S.; Pulpipat, T.; Wang, P.; Chen, S. Comparison of the pathogenicity of *Francisella orientalis* in Nile tilapia (*Oreochromis niloticus*), Asian seabass (*Lates calcarifer*) and largemouth bass (*Micropterus salmoides*) through experimental intraperitoneal infection. *J. Fish Dis.* **2020**, *43*, 1097–1106. [[CrossRef](#)]
68. Duodu, S.; Larsson, P.; Sjödin, A.; Forsman, M.; Colquhoun, D.J. The distribution of francisella-like bacteria associated with coastal waters in Norway. *Microb. Ecol.* **2012**, *64*, 370–377. [[CrossRef](#)]
69. Berrada, Z.L.; Telford, S.R. Diversity of *Francisella* Species in Environmental Samples from Martha’s Vineyard, Massachusetts. *Microb. Ecol.* **2010**, *59*, 277–283. [[CrossRef](#)]
70. Seshadri, R.; Paulsen, I.T.; Eisen, J.A.; Read, T.D.; Nelson, K.E.; Nelson, W.C.; Ward, N.L.; Tettelin, H.; Davidsen, T.M.; Beanan, M.J.; et al. Complete genome sequence of the Q-fever pathogen *Coxiella burnetii*. *Proc. Natl. Acad. Sci. USA* **2003**, *100*, 5455–5460. [[CrossRef](#)]
71. Wu, S.; Tian, J.; Gatesoupe, F.; Li, W.; Zou, H.; Yang, B.; Wang, G. Intestinal microbiota of gibel carp (*Carassius auratus gibelio*) and its origin as revealed by 454 pyrosequencing. *World J. Microbiol. Biotechnol.* **2013**, *29*, 1585–1595. [[CrossRef](#)]
72. Peng, W.; Li, X.; Lin, M.; Fan, W. Microbiological analysis of cadmium-contaminated sediments during biostabilization with indigenous sulfate-reducing bacteria. *J. Soil. Sediment.* **2020**, *20*, 584–593. [[CrossRef](#)]
73. Boeraş, I.; Burcea, A.; Coman, C.; Bănăduc, D.; Curtean-Bănăduc, A. Bacterial microbiomes in the sediments of lotic systems ecologic drivers and role: A case study from the Mures River, Transylvania, Romania. *Water-Sui.* **2021**, *13*, 3518. [[CrossRef](#)]
74. Huang, W.; Chen, X.; Wang, K.; Chen, J.; Zheng, B.; Jiang, X. Comparison among the microbial communities in the lake, lake wetland, and estuary sediments of a plain river network. *MicrobiologyOpen* **2019**, *8*, e644. [[CrossRef](#)]

75. Sikorski, J.; Möhle, M.; Wackernagel, W. Identification of complex composition, strong strain diversity and directional selection in local *Pseudomonas stutzeri* populations from marine sediment and soils. *Environ. Microbiol.* **2002**, *4*, 465–476. [[CrossRef](#)]
76. Chen, Q.; Li, Y.; Liu, M.; Zhu, B.; Mu, J.; Chen, Z. Removal of Pb and Hg from marine intertidal sediment by using rhamnolipid biosurfactant produced by a *Pseudomonas aeruginosa* strain. *Environ. Technol. Innov.* **2021**, *22*, 101456. [[CrossRef](#)]
77. Park, Y.; Ko, J.; Yun, S.; Lee, E.Y.; Kim, S.; Kang, S.; Lee, B.; Kim, S. Enhancement of bioremediation by *Ralstonia* sp. HM-1 in sediment polluted by Cd and Zn. *Bioresour. Technol.* **2008**, *99*, 7458–7463. [[CrossRef](#)]
78. Urbanczyk, H.; Ast, J.C.; Dunlap, P.V. Phylogeny, genomics, and symbiosis of *Photobacterium*. *FEMS Microbiol. Rev.* **2011**, *35*, 324–342. [[CrossRef](#)]
79. Kim, M.; Cha, I.; Lee, K.; Lee, E.; Park, S. Genomics reveals the metabolic potential and functions in the redistribution of dissolved organic matter in marine environments of the genus *Thalassotalea*. *Microorganisms* **2020**, *8*, 1412. [[CrossRef](#)]
80. Zhang, X.; Xu, W.; Liu, Y.; Cai, M.; Luo, Z.; Li, M. Reveals microbial diversity and metabolic potentials of seawater and surface. *Front. Microbiol.* **2018**, *9*, 2402. [[CrossRef](#)]
81. Mikhailov, I.S.; Zakharova, Y.R.; Bukin, Y.S.; Galachyants, Y.P.; Petrova, D.P.; Sakirko, M.V.; Likhoshway, Y.V. Co-occurrence networks among bacteria and microbial eukaryotes of lake Baikal during a spring phytoplankton bloom. *Microb. Ecol.* **2019**, *77*, 96–109. [[CrossRef](#)]
82. Kurm, V.; van der Putten, W.H.; Weidner, S.; Geisen, S.; Snoek, B.L.; Bakx, T.; Hol, W.H.G. Competition and predation as possible causes of bacterial rarity. *Environ. Microbiol.* **2019**, *21*, 1356–1368. [[CrossRef](#)] [[PubMed](#)]
83. Hu, S.; He, R.; Wang, W.; Zhao, D.; Zeng, J.; Huang, R.; Duan, M.; Yu, Z. Composition and co-occurrence patterns of *Phragmites australis* rhizosphere bacterial community. *Aquat. Ecol.* **2021**, *55*, 695–710. [[CrossRef](#)]
84. Yuan, Q.; Wang, P.; Wang, X.; Hu, B.; Tao, L. Phytoremediation of cadmium-contaminated sediment using *Hydrilla verticillata* and *Elodea canadensis* harbor two same keystone rhizobacteria *Pedospaeraceae* and *Parasegetibacter*. *Chemosphere* **2022**, *286*, 131648. [[CrossRef](#)] [[PubMed](#)]
85. Kett, G.F.; Culloty, S.C.; Jansen, M.A.K.; Lynch, S.A. Development of a sensitive polymerase chain reaction (PCR) and digoxigenin (DIG)-labeled in situ hybridization (ISH) for the detection of *Vibrio* bacteria in the Pacific oyster *Crassostrea gigas*. *Aquac. Rep.* **2022**, *22*, 100961. [[CrossRef](#)]
86. Möller, L.; Kreikemeyer, B.; Luo, Z.; Jost, G.; Labrenz, M. Impact of coastal aquaculture operation systems in Hainan island (China) on the relative abundance and community structure of *Vibrio* in adjacent coastal systems. *Estuar. Coast. Shelf Sci.* **2020**, *233*, 106542. [[CrossRef](#)]
87. Jung, S.W.; Kang, J.; Park, J.S.; Joo, H.M.; Suh, S.; Kang, D.; Lee, T.; Kim, H. Dynamic bacterial community response to *Akashiwo sanguinea* (Dinophyceae) bloom in indoor marine microcosms. *Sci. Rep.* **2021**, *11*, 6983. [[CrossRef](#)] [[PubMed](#)]
88. Zhang, J.; Chen, M.; Jiafeng, H.; Guo, X.; Zhang, Y.; Liu, D.; Wu, R.; He, H.; Wang, J. Diversity of the microbial community and cultivable protease-producing bacteria in the sediments of the Bohai Sea, Yellow Sea and South China Sea. *PLoS ONE* **2019**, *14*, e215328. [[CrossRef](#)]
89. Liang, S.; Deng, J.; Jiang, Y.; Wu, S.; Zhou, Y.; Zhu, W. Functional distribution of bacterial community under different land use patterns based on FaProTax function prediction. *Pol. J. Environ. Stud.* **2020**, *29*, 1–17. [[CrossRef](#)]
90. Lin, G.; Lin, X. Bait input altered microbial community structure and increased greenhouse gases production in coastal wetland sediment. *Water Res.* **2022**, *218*, 118520. [[CrossRef](#)]
91. Lee, Y.; Choi, Y. Complete genome sequence and analysis of three kinds of  $\beta$ -agarase of *Cellulophaga lytica* DAU203 isolated from marine sediment. *Mar. Genom.* **2017**, *35*, 43–46. [[CrossRef](#)]
92. Shi, P.; Wang, H.; Feng, M.; Cheng, H.; Yang, Q.; Yan, Y.; Xu, J.; Zhang, M. The coupling response between different bacterial metabolic functions in water and sediment improve the ability to mitigate climate change. *Water* **2022**, *14*, 1203. [[CrossRef](#)]
93. Nielsen, L.P.; Risgaard-Petersen, N. Rethinking sediment biogeochemistry after the discovery of electric currents. *Annu. Rev. Mar. Sci.* **2015**, *7*, 425–442. [[CrossRef](#)] [[PubMed](#)]
94. Zhu, W.; Qin, C.; Ma, H.; Xi, S.; Zuo, T.; Pan, W.; Li, C. Response of protist community dynamics and co-occurrence patterns to the construction of artificial reefs: A case study in Daya Bay, China. *Sci. Total Environ.* **2020**, *742*, 140575. [[CrossRef](#)] [[PubMed](#)]